Mitochondrial calcium uniporter promotes mitophagy by regulating the PINK1/Parkin pathway in caerulein-treated pancreatic ductal epithelial cells *in vitro*

YU LEI*, HUI-YING YANG*, NUO MENG, YING-YING QIN, MENG-TAO XU, XUE-LIAN XIANG, LI LIU and GUO-DU TANG

Department of Gastroenterology, The First Affiliated Hospital of Guangxi Medical University, Nanning, Guangxi 530021, P.R. China

Received July 14, 2023; Accepted February 2, 2024

DOI: 10.3892/etm.2024.12435

Abstract. The mitochondrial calcium uniporter (MCU) is a major protein for the uptake of mitochondrial calcium to regulate intracellular energy metabolism, including processes such as mitophagy. The present study investigated the effect of the MCU on mitophagy in pancreatic ductal epithelial cells (PDECs) in acute pancreatitis (AP) *in vitro*. The normal human PDECs (HPDE6-C7) were treated with caerulein (CAE) to induce AP-like changes, with or without ruthenium red to inhibit the MCU. The mitochondrial membrane potentials (MMPs) and mitochondrial Ca^{2+} levels were analyzed by fluorescence. The expression levels of MCU, LC3, p62, and translocase of the outer mitochondrial membrane complex subunit 20 (TOMM20), putative kinase 1 (PINK1), and Parkin were measured by western blotting and immunofluorescence. Mitophagy was observed by confocal fluorescence microscopy and transmission electron microscopy. The results showed that CAE increased the MCU protein expression, mitochondrial Ca^{2+} levels, MMP depolarization and the protein expression of mitophagy markers including the LC3II/I ratio, PINK1, and Parkin. CAE decreased the protein expression of p62 and TOMM20, and promoted the formation of mitophagosomes in HPDE6-C7 cells. Notably, changes in these markers were reversed by inhibiting the MCU. In conclusion, an activated MCU may promote mitophagy by regulating the PINK1/Parkin pathway in PDECs in AP.

Correspondence to: Professor Guo-Du Tang, Department of Gastroenterology, The First Affiliated Hospital of Guangxi Medical University, 6 Shuangyong Road, Nanning, Guangxi 530021, P.R. China
E-mail: tangguodu@stu.gxmu.edu.cn

*Contributed equally

Key words: mitochondrial calcium uniporter, mitophagy, putative kinase 1/Parkin pathway, pancreatic ductal epithelial cells, acute pancreatitis

Introduction

Acute pancreatitis (AP) is characterized by pancreatic acinar cell death and persistent local or systemic inflammation. The incidence of the disease is increasing and the mortality is high (1). Currently, the complex pathogenesis of AP is still unclear. Studies have confirmed that mitochondrial Ca^{2+} overload is associated with acinar cell death in AP (2,3). However, most of the current studies regarding the pathogenesis of AP primarily focus on acinar cells, while only a few studies focus on pancreatic ductal epithelial cells (PDECs), which is another important cell type closely related to AP.

PDECs play a key role in maintaining pancreatic homeostasis and avoiding substantial pancreatic inflammation (4-6). Studies have shown that transient high pressure, intracellular Ca^{2+} overload, and cytoskeletal changes of PDECs can aggravate AP (7-9). In addition, PDECs are an important component of the pancreatic ductal mucosal barrier (PDMB) and play an important role in preventing abnormal activation of trypsinogen and the reflux of digestive enzymes to the pancreas (5,10). Furthermore, impaired ductal fluid secretion and a lower intraluminal pH lead to zymogen activation and acinar cell dysfunction (11,12). Therefore, the decrease of PDMB function caused by PDECs damage may be the main cause of pancreatic injury and AP occurrence. Studying PDECs will help to uncover the underlying mechanisms of the development of AP.

A previous study from our group has identified intracellular Ca^{2+} overload in PDECs in AP (9). As one of the most important intracellular signal transduction molecules, Ca^{2+} is involved in almost every physiological activity within cells, including mitophagy. Mitophagy is the selective autophagy of mitochondria whereby dysfunctional mitochondria are transported to lysosomes for degradation (13) and it has a crucial role in mitochondrial quality and quantity control as well as cell survival. Mitochondrial Ca^{2+} overload is related to the mitochondrial structure, mitochondrial reactive oxygen species, mitochondrial membrane potential (MMP), and ATP production, which all contribute to the initiation of mitophagy (14).

Recent studies have shown that mitophagy within pancreatic acinar cells plays an important role in the pathogenesis and

development of AP. This includes both PTEN-induced putative kinase 1 (PINK1)/Parkin-activated mitophagy and vacuole membrane protein 1-related mitophagy (15,16). However, whether similar mechanisms exist in PDECs remains to be elucidated. Intracellular Ca^{2+} overload in acinar cells leads to mitochondrial depolarization through the opening of the mitochondrial permeability transition pore (17) and these damaged mitochondria can be removed by mitophagy. However, the relationship between mitochondrial Ca^{2+} overload and mitophagy in PDECs during AP has not been investigated.

The mitochondrial calcium uniporter (MCU), as a highly selective Ca^{2+} uptake channel, transports Ca^{2+} into the mitochondrial matrix along an electrochemical gradient (18). As such, the MCU plays a crucial role in mitochondrial Ca^{2+} homeostasis and mitochondrial energy metabolism. There has been convincing evidence to suggest a close relationship between the MCU and mitophagy. Guan *et al* (19) found that upregulation of the MCU inhibited mitochondrial fusion and mitophagy through the calpain/optic atrophy type 1 signaling pathway, leading to myocardial ischemia-reperfusion injury. Chen *et al* (20) found that proliferation stimulated by apelin-13 in vascular smooth muscle cells was regulated by mitophagy that was caused by MCU-associated mitochondrial Ca^{2+} uptake. The MCU may be a key protein that links mitochondrial Ca^{2+} overload and mitophagy. A previous study by our group indicated that MCU expression and mitochondrial Ca^{2+} were increased in the rat model of AP (21). However, the exact mechanism by which MCU regulates mitophagy through mitochondrial Ca^{2+} regulation in AP remains to be elucidated.

Caerulein (CAE), an analog of cholecystokinin, has been widely used *in vitro* and *in vivo* to establish models of AP (22). Our previous studies found that the change in protein expression of autophagy marker, the apoptosis and pyroptosis protein expression of NLPR3, cleaved caspase-1 and cleaved caspase-3, the tight junction protein expression of ZO-1 and occludin in HPDE6-C7 cells treated with CAE *in vitro* were consistent with the rat model of AP (8,9,23,24). In the present study, it was hypothesized that MCU-associated mitochondrial Ca^{2+} overload promotes mitophagy by regulating the PINK1/Parkin pathway in AP. To test this hypothesis, CAE-treated HPDE6-C7 cells were used to imitate the pathological changes of PDECs in AP. In addition, ruthenium red (RR) is an inorganic polycationic dye that has been reported as an MCU inhibitor (25). It was first used to stain specific plant material and was subsequently found to be a voltage-sensitive calcium channel inhibitor (26,27). Therefore, RR was used as an MCU-specific inhibitor to assess the effect of MCU on mitophagy in the present study.

Materials and methods

Cell culture. Normal human pancreatic ductal epithelial cells (HPDE6-C7) were obtained from WHELAB (https://www.whelab.com/pro/580.html; cat. no. C1248; passage 3) and cultured in Dulbecco's Modified Eagle's Medium (DMEM; cat. no. C11995500BT; Gibco; Thermo Fisher Scientific, Inc.) supplemented with 10% fetal bovine serum (cat. no. S711-001S; Shanghai Shuangru Biotechnology Co., Ltd.), 100 U/ml penicillin, and 0.1 mg/ml streptomycin (cat. no. P1400; Beijing Solarbio Science & Technology Co., Ltd.). Cells were placed in an incubator with sterile humidified air with 5% CO_2 at 37˚C. Cells were treated at the same time with CAE (100 nmol/l; cat. no. EY5113; Shanghai Amquar Biological Technology Co., Ltd.) and RR (10 μmol/l; cat. no. 00541; MilliporeSigma) for 24 h. CAE and RR were both dissolved in phosphate-buffered saline for the experiments. Cells were divided into four groups according to the type of treatment: CAE, RR, CAE+RR, and control.

Flow cytometry. Following treatment with RR (1, 5, 10, 50 and 100 μmol/l) for 24 h, the rate of apoptosis in HPDE6-C7 cells was detected using the annexin V-FITC/PI kit [cat. no. AT101; Multisciences (Lianke) Biotech Co., Ltd.], following the manufacturer's instructions. In brief, after digestion with an accutase solution, the cells were resuspended in binding buffer, then incubated with 5 μl of annexin V-FITC and 10 μl of PI for 5 min at 25˚C in an incubator. Cell apoptosis rates were calculated as the percentage of early + late apoptotic cells and measured by flow cytometry (FACSVerse, BD Biosciences) and scatter diagrams were visualized using FlowJo software version 10.8.1 (FlowJo LLC).

Cell Counting Kit (CCK-8) assay. HPDE6-C7 cells were plated in a 96-well plate and cultured for 6 h. After treatment with RR (1, 5, 10, 50 and 100 μmol/l) for 24 h at 37˚C, the cell medium was replaced with a mixture of fresh medium (90%) and CCK-8 reagent (10%). Cells were incubated for 1 h at 37˚C in the dark, and the absorbance was measured at 450 nm.

Western blotting. Protein was isolated from HPDEE6-C7 cells using RIPA lysis buffer (cat. no. R0020; Beijing Solarbio Science & Technology Co., Ltd.) supplemented with 1 mmol/l PMSF, and the protein concentration was measured by a BCA Protein Assay Kit (cat. no. P0012; Beyotime Institute of Biotechnology). Equivalent amounts of protein (50 μg/well) were separated by 10 or 15% SDS-PAGE. The gels were electroblotted onto PVDF membranes (162-0219; Bio-Rad Laboratories, Inc.). Next, membranes were placed in nonfat milk (cat. no. P0216; Beyotime Institute of Biotechnology) for 40 min at room temperature and incubated at 4˚C for 16-20 h with primary antibodies, including: MCU (cat. no. 14997S; Cell Signaling Technology, Inc.; 1:1,000), LC3 (cat. no. ab48394; Abcam; 1:1,000), SQSTM1/p62 (cat. no. ab109012; Abcam; 1:15,000), and translocase of the outer mitochondrial membrane complex subunit 20 (cat. no. TOMM20; ab186735; Abcam; 1:2,000), PINK1 (cat. no. ab300623; Abcam; 1:1,000), Parkin (cat. no. 14060-1-AP; Proteintech Group, Inc.; 1:1,000), β-Actin (cat. no. 4970S; Cell Signaling Technology, Inc.; 1:1,000), and GAPDH (cat. no. ab9485; Abcam; 1:2,500). The following day, the membranes were incubated with the DyLight 800-conjugated secondary anti-rabbit antibody for 1 h at room temperature (cat. no. 5151; Cell Signaling Technology, Inc.; 1:10,000). Proteins were visualized using the Odyssey infrared imaging system (LI-COR, Inc.), and the gray value of the protein band was analyzed using ImageJ software (version 1.53e; National Institutes of Health).

Transmission electron microscopy (TEM). HPDE6-C7 cells were immersed in electron microscope fixation fluid for 2.5 h at 4˚C for fixation and stained in 1% osmium acid for 2 h at

room temperature. After dehydration, cells were embedded in epoxy resin at 37˚C overnight. Epoxy resin samples were heated at 60˚C for 48 h, and slices (80 nm) were obtained using an ultramicrotome (EM UC7; Leica Microsystems GmbH). After counterstaining sequentially with 2% uranium acetate and 2.6% lead citrate for 8 min at room temperature, images were observed by TEM (HT7700; Hitachi High-Technologies Corporation).

Measurement of mitochondrial membrane potentials (MMP). MMP changes in HPDE6-C7 cells were measured with an MMP assay kit and JC-1 (cat. no. C2006; Beyotime Institute of Biotechnology). Briefly, cells were loaded with the JC-1 working solution (X1) at 37˚C for 20 min. After washing with pre-cooled staining buffer, cells were immediately observed using fluorescence microscopy (Olympus Corporation). Fluorescent images were analyzed using ImageJ software (version 1.53e; National Institutes of Health).

Measurement of mitochondrial Ca^{2+}. Levels of mitochondrial Ca^{2+} in HPDE6-C7 cells were identified using Rhod-2 AM (cat. no. 40776ES50, Shanghai Yeasen Biotechnology Co., Ltd.) and Mito-Tracker Green (MTG; cat. no. C1048; Beyotime Institute of Biotechnology). After washing with D-Hank's balanced salt solution (cat. no. H1046; Beijing Solarbio Science & Technology Co., Ltd.), cells were loaded with the Rhod-2 AM working solution (4 μmol/l) at 37˚C for 30 min. Subsequently, cells were loaded with MTG (200 nmol/l) at 37˚C for 30 min and immediately observed with a fluorescence microscope (Olympus Corporation). Fluorescent images were analyzed using ImageJ software (version 1.53e; National Institutes of Health).

Fluorescence colocalization assay of mitochondria and lysosomes. To visualize the formation of autolysosomes during mitophagy, MTG and Lyso-Tracker Red (LTR; cat. no. C1046; Beyotime Institute of Biotechnology) were used to label the mitochondria and lysosomes, respectively. Cells were cultured in confocal dishes (BS-15-GJM, Biosharp) and stained in medium containing 200 nmol/l MTG for 30 min and 75 nmol/l LTR for 15 min at 37˚C. Confocal fluorescent images were obtained using a laser scanning confocal microscope (TCS SP8 STED; Leica Microsystems GmbH) with a x63 oil immersion objective.

Immunofluorescence. At room temperature, HPDE6-C7 cells were fixed in 4% paraformaldehyde for 15 min, then permeabilized with 0.1% Triton X-100 for 5 min. After treatment with blocking buffer for 30 min, cells were incubated at 4˚C overnight with primary antibodies, including LC3 (cat. no. ab48394; Abcam; 1:1,000), Parkin (cat. no. 14060-1-AP; Proteintech Group, Inc.; 1:500), and TOMM20 (cat. no. 66777-1-Ig; Proteintech Group, Inc.; 1:500). Subsequently, cells were incubated with Alexa Fluor 555 (cat. no. 4413S; Cell Signaling Technology, Inc.; 1:1,000) and Alexa Fluor 488 (cat. no. 550036, Chengdu Zen-Bioscience Co., Ltd.; 1:1,000)-conjugated secondary antibodies for 1 h at room temperature in the dark. Fluorescent images were obtained using a fluorescence microscope (Carl Zeiss AG).

Statistical analysis. All experiments were repeated at least three times. Data were presented as the mean ± standard deviation, and SPSS 26 software (IBM Corp.) was used to perform all statistical analyses. Pearson's correlation coefficient (PCC) was determined as a statistic for quantifying colocalization using the ImageJ plugin Colocalization Finder. Student's *t*-test or one-way analysis of variance followed by Tukey's test was used to determine the statistical significance between indicated groups. $P<0.05$ was considered to indicate a statistically significant difference. Cartograms were generated using GraphPad Prism 9 software (Dotmatics).

Results

RR inhibited MCU expression in CAE-treated HPDE6-C7 cells. RR has been reported as a specific inhibitor of MCU (28). To identify a working nontoxic concentration of RR for the current study, the cytotoxic effect of RR in HPDE6-C7 cells was evaluated using a CCK-8 assay and flow cytometry. The results of the CCK-8 assay revealed decreased cell viability with higher concentrations of RR (50 or 100 μmol/l; Fig. 1A). Flow cytometry also confirmed that apoptosis was increased in cells exposed to 50 or 100 μmol/l RR (Fig. 1B and C). Thus, the maximum nontoxic concentration of RR (10 μmol/l) was used in subsequent experiments. Additionally, western blotting revealed that CAE increased the expression level of MCU and RR treatment restrained MCU expression in CAE-treated cells (Fig. 1D and E).

Inhibition of MCU attenuated CAE-induced mitochondrial Ca^{2+} accumulation and MMP decline in HPDE6-C7 cells. The effect of CAE on mitochondrial Ca^{2+} levels and MMP in HPDE6-C7 cells was explored using fluorescence microscopy. The results of PCC indicated that the Rhod-2-loaded Ca^{2+} were strongly correlated with the Mito-Tracker (Fig. 2C). Therefore, it can be speculated that the Rhod-2-loaded Ca^{2+} may come from mitochondria. The results indicated that treatment of HPDE6-C7 cells with CAE overtly increased mitochondrial Ca^{2+} accumulation (Fig. 2A and B). Furthermore, cells were loaded with JC-1 to measure the MMP. The red/green fluorescence density was decreased in CAE-treated cells, indicating that treatment with CAE induced MMP depolarization (Fig. 2D and E). Notably, RR effectively attenuated mitochondrial Ca^{2+} accumulation and restored MMP in CAE-treated cells. These data demonstrated that CAE promotes MCU-associated mitochondrial Ca^{2+} overload and MMP decline.

Inhibition of MCU attenuated CAE-induced mitophagy in HPDE6-C7 cells. The effect of MCU on mitophagy in AP was investigated by western blotting, immunofluorescence, fluorescence probes and TEM. The results of western blotting indicated that CAE improved the LC3-II/I ratio and reduced the expression of p62 and TOMM20. In turn, the LC3-II/I ratio was reduced and the expression of p62 and TOMM20 were increased by RR treatment in CAE-treated cells (Fig. 3A and B). In addition, the results of the immunofluorescence assays showed that the colocalization of LC3 and TOMM20 was increased in the CAE-treated cells, but this increased colocalization was decreased by treating the

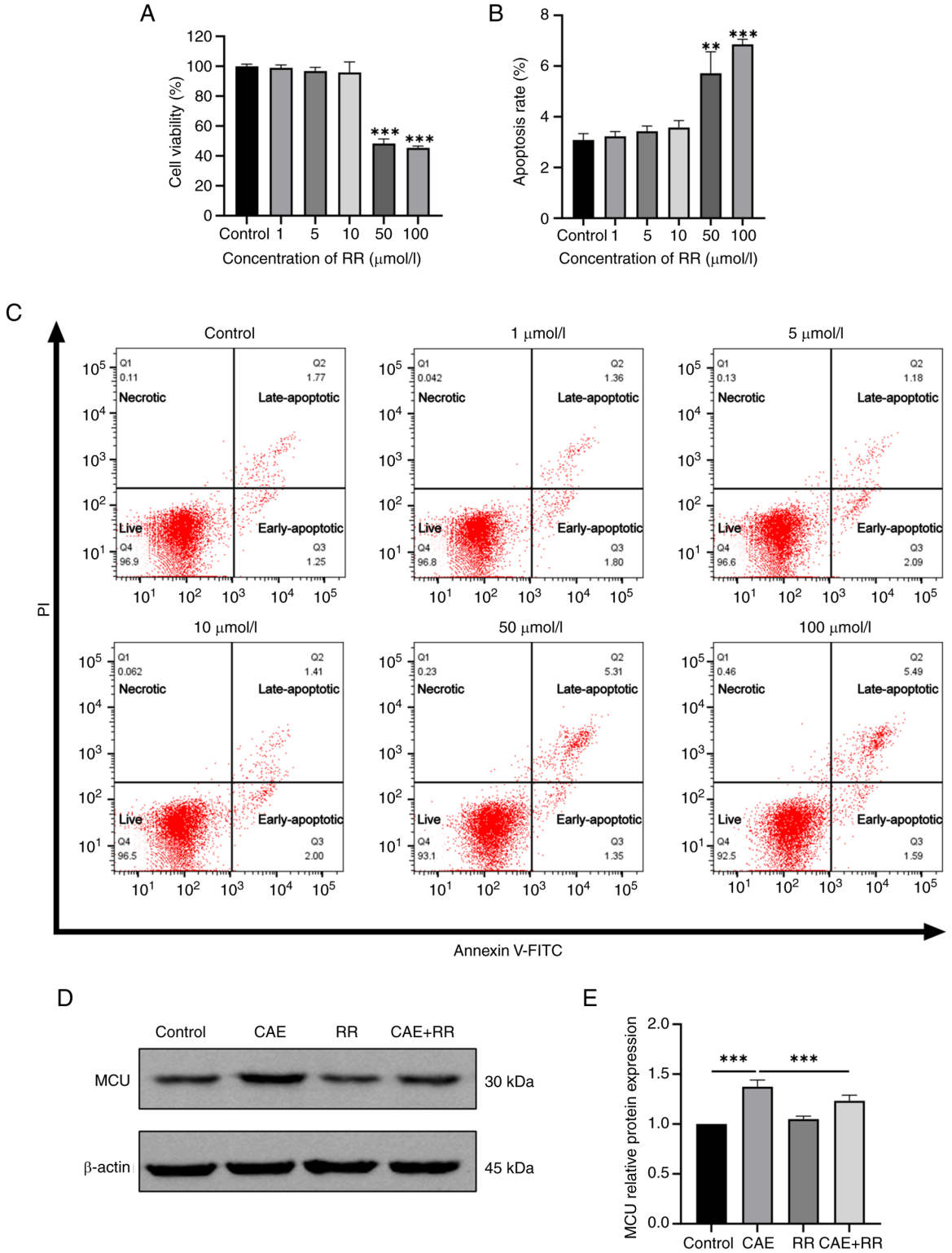

Figure 1. Effects of RR on the viability and apoptosis of HPDE6-C7 cells, and MCU expression in CAE-treated HPDE6-C7 cells. HPDE6-C7 cells were treated with RR (1, 5, 10, 50 and 100 μmol/l) for 24 h. (A) CCK-8 assay was used to detect cell viability. (B and C) Cell apoptosis was detected by flow cytometry. Q1: Necrotic cells, Q2: Late-apoptotic cells, Q3: Early-apoptotic cells, Q4: Live cells. HPDE6-C7 cells were treated with 10 μmol/l RR and 100 nmol/l CAE for 24 h. (D) Western blot and (E) semiquantitative analysis of MCU expression. Data were presented as the mean ± standard deviation. **P<0.01, ***P<0.001 vs. control. All experiments were repeated at least three times. RR, ruthenium red; MCU, mitochondrial calcium uniporter; CAE, caerulein.

cells with RR (Fig. 3C and D). Moreover, the fluorescence images showed that the colocalization of mitochondria and lysosomes was increased in CAE-treated cells, which indicate an increased fusion of mitophagosomes and lysosomes. However, RR treatment reduced the overlap of mitochondrial and lysosomal staining (Fig. 4A and B). Furthermore, autophagosomes during mitophagy and impaired mitochondria were also detected by TEM and RR treatment reduced the formation of mitophagosomes and damaged mitochondria (Fig. 4C). These results demonstrated that

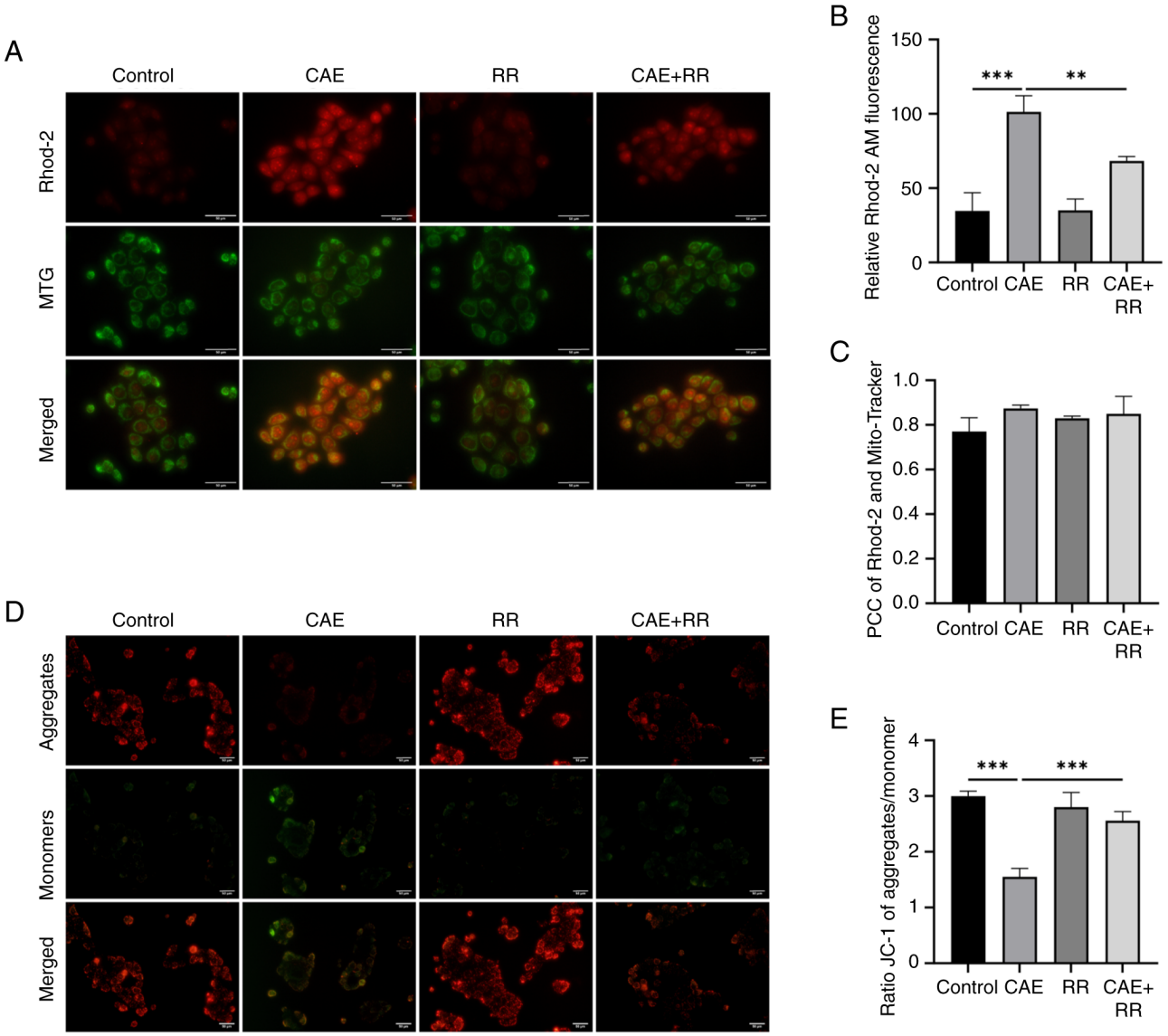

Figure 2. RR treatment inhibited mitochondrial Ca^{2+} accumulation and reduced MMP decline in HPDE6-C7 cells. HPDE6-C7 cells were treated with 10 μmol/l RR and 100 nmol/l CAE for 24 h. (A and B) Changes in mitochondrial Ca^{2+} were detected by labeling with Rhod-2 AM and MTG and observed under a fluorescence microscope (magnification, x400; scale bar, 50 μm). (C) PCC was used to calculate the correlation between Rhod-2 AM and MTG. No correlation: PCC=0; weak: PCC <0.4; moderate: 0.4 ≤PCC <0.7; strong: 0.7 ≤PCC<1; complete or perfect: PCC=1. (D and E) Changes in MMP were detected by staining with JC-1 and observation under a fluorescence microscope (magnification, x200; scale bar, 50 μm). Data were presented as the mean ± standard deviation. **P<0.01, ***P<0.001 vs. control. All experiments were repeated at least three times. RR, ruthenium red; MMP, mitochondrial membrane potential; CAE, caerulein; MTG, Mito-Tracker Green; PCC, Pearson's correlation coefficient.

elevated mitophagy in CAE-treated cells can be reduced by RR treatment.

Inhibition of MCU attenuated PINK1/Parkin pathway activation in HPDE6-C7 cells. The effect of MCU on the PINK1/Parkin pathway in AP was investigated by western blotting and immunofluorescence. The results of western blotting showed that CAE increased the expression of PINK1 and Parkin, but this increased expression could be reversed by treating the cells with RR (Fig. 5A and B). Moreover, the immunofluorescence of Parkin and TOMM20 indicated that the expression of Parkin was increased in CAE-treated cells, demonstrating that CAE promoted the translocation of Parkin into the mitochondrial membrane. As expected, this effect was alleviated by RR treatment (Fig. 5C).

Discussion

Previous studies have confirmed that mitophagy is involved in the pathogenesis of AP (15,29,30). In addition, MCU-associated mitochondrial Ca^{2+} overload plays a key role in AP (31,32). However, the effect of MCU on mitophagy in AP remains ambiguous. The present study was the first to investigate the regulatory role of MCU on mitophagy in AP, to the best of the authors' knowledge. The data indicate that activated MCU may promote mitophagy by regulating the PINK1/Parkin pathway in PDECs in AP *in vitro*.

Studies have demonstrated that mitochondrial Ca^{2+} overload plays a crucial role in the initiation of acinar cell death in AP (2,3,17). As an essential channel for mitochondrial Ca^{2+} uptake, the MCU may play an important role during

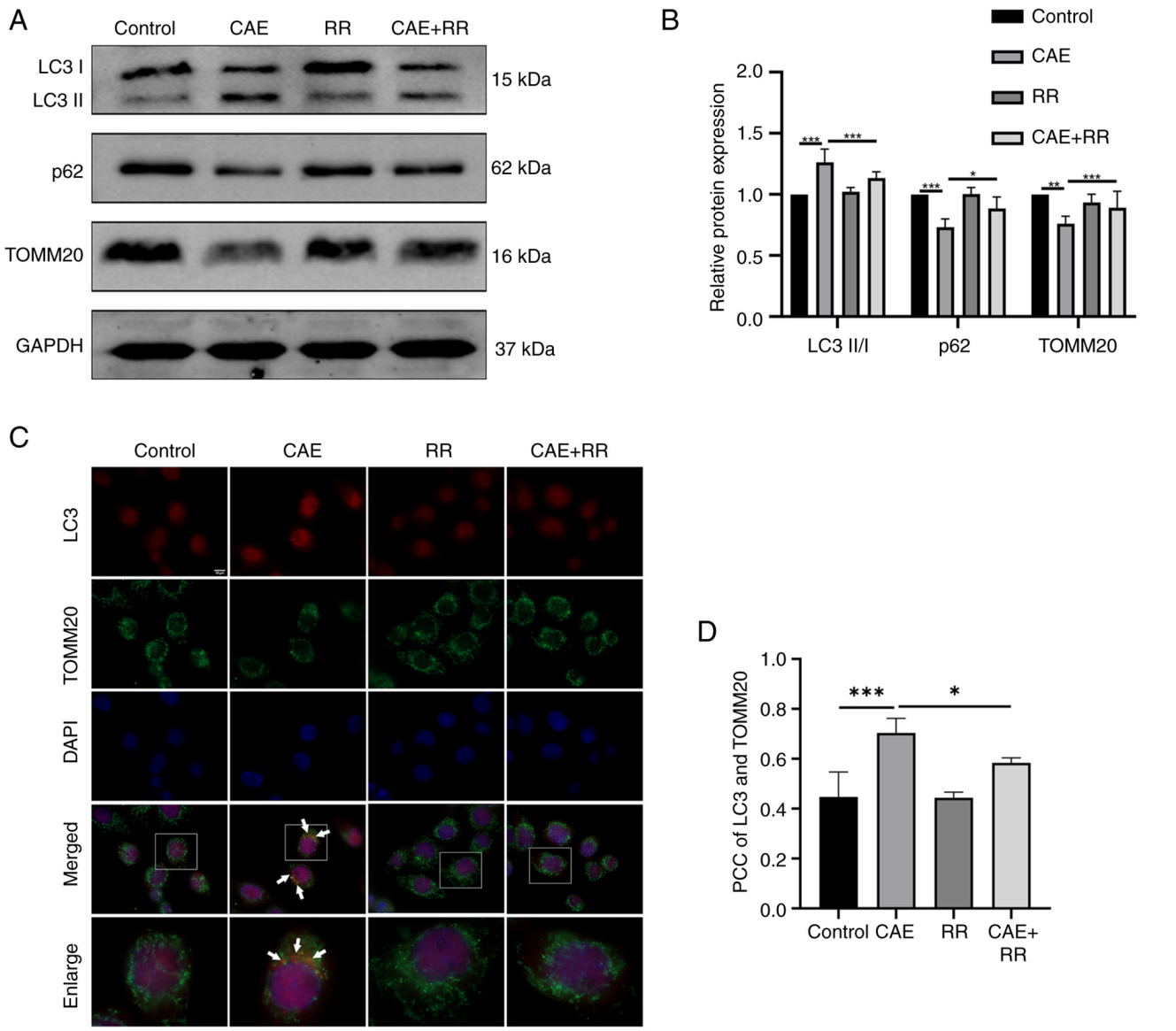

Figure 3. RR treatment inhibited CAE-induced mitophagy in HPDE6-C7 cells. HPDE6-C7 cells were treated with 10 μmol/l RR and 100 nmol/l CAE for 24 h. (A and B) Expression of microtubule-associated proteins 1A/1B LC3B, p62 and TOMM20 were detected by western blotting. (C and D) TOMM20 (a mitochondrial marker) colocalization with LC3 was observed by fluorescence microscopy (magnification, x1,000; scale bar, 10 μm). The PCC was used to calculate the colocalization between LC3 and TOMM20. No correlation: PCC=0; weak: PCC <0.4; moderate: 0.4 ≤PCC <0.7; strong: 0.7 ≤PCC<1; complete or perfect: PCC=1. Data were presented as the mean ± standard deviation. *P<0.05, **P<0.01, ***P<0.001 vs. control. All experiments were repeated at least three times. RR, ruthenium red; CAE, caerulein; TOMM20, translocase of the outer mitochondrial membrane complex subunit 20; PCC, Pearson's correlation coefficient.

mitophagy in AP. The results in the present study showed that CAE increased MCU overexpression, mitochondrial Ca^{2+} accumulation, and MMP depolarization. RR is a potent inhibitor of MCU (33). In the present study, the inhibition of the MCU by RR efficiently attenuated mitochondrial Ca^{2+} accumulation and restored MMP depolarization. These results demonstrated that reducing MCU-dependent mitochondrial Ca^{2+} uptake could improve MMP depolarization in PEDCs in AP. Notably, RR could not decrease the mitochondrial Ca^{2+} level in normal cells in the present study. Similarly, in our previous study of AP in rats, RR inhibited mitochondrial Ca^{2+} overload in the AP group, but did not reduce mitochondrial Ca^{2+} in the control group (21). Moreover, in Jiang *et al* (34), RR inhibited mitochondrial Ca^{2+} overload promoted by aconitine, but did not reduce mitochondrial Ca^{2+} in mouse hippocampal neuron HT22 cells. These phenomena may be due to the fact that RR does not interfere with the cytoplasmic Ca^{2+} signal propagation to the mitochondria in normal cells (27). In addition, the gating of MCU by the mitochondrial calcium uptake 1 may have a barrier effect on RR in normal cells (35).

Mitochondrial dysfunction and mitophagy have been extensively studied in acinar cells in AP (17,36,37). However, the presence of mitophagy in PDECs in AP and its underlying mechanisms remain unclear. LC3-II as a molecular marker of autophagy represents the relative number of autophagosomes and p62 as an autophagy substrate is negatively correlated with autophagy (38-40). A reduction in the expression of TOMM20, which is a translocase of the outer mitochondrial membrane 20, indicates that impaired mitochondria may be removed by mitophagy. Our previous study found that CAE induced autophagy activation in the early stage of AP (8). RR mainly inhibits mitochondrial Ca^{2+} and is recognized as a

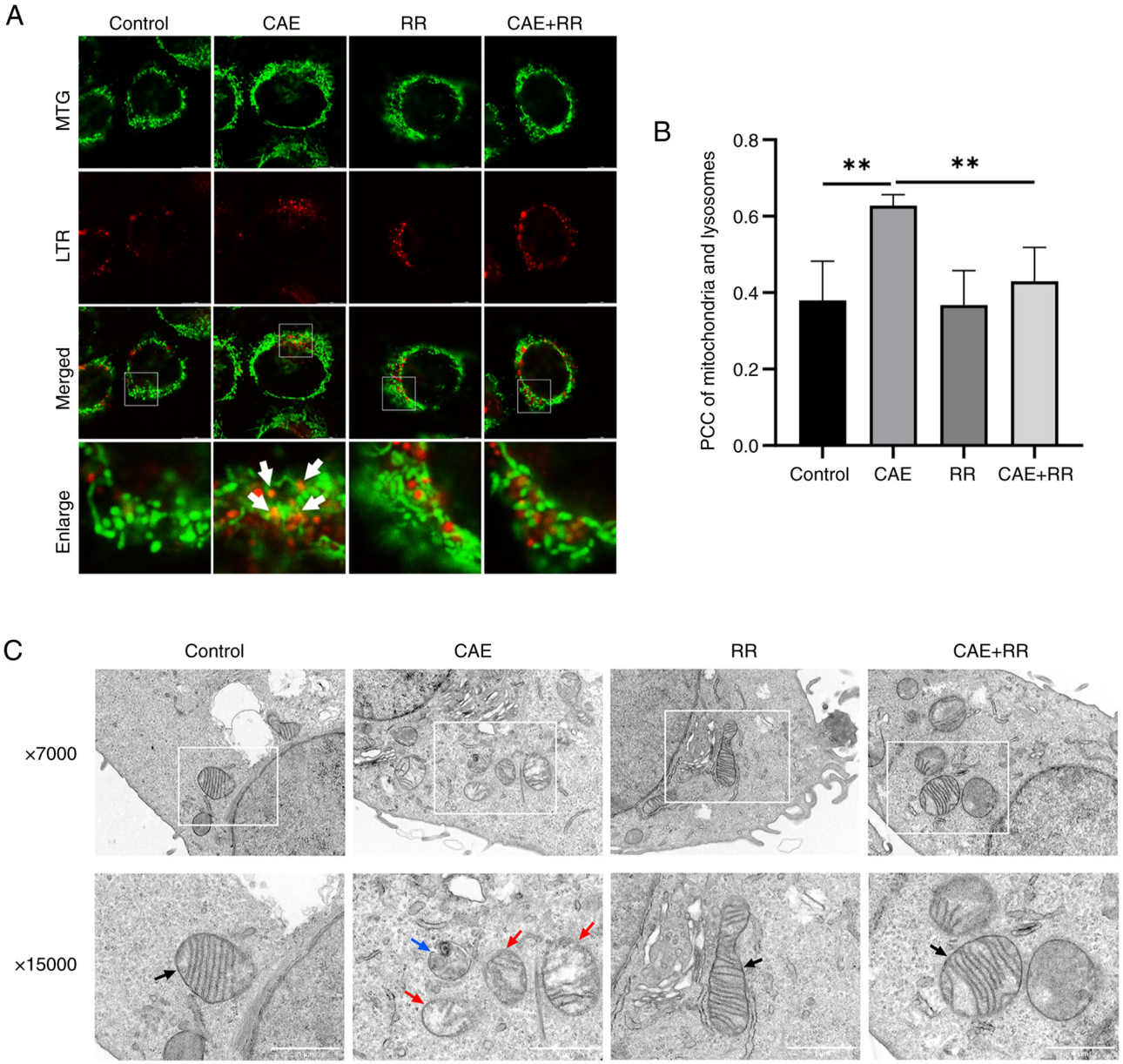

Figure 4. RR treatment reduced CAE-induced mitophagosome formation in HPDE6-C7 cells. (A and B) Mitochondrial colocalization with lysosomes was observed by fluorescence confocal microscopy (magnification, x630; scale bar, 10 μm). The PCC was used to calculate the colocalization between mitochondria and lysosomes. No correlation: PCC=0; weak: PCC <0.4; moderate: 0.4 ≤PCC <0.7; strong: 0.7 ≤PCC<1; complete or perfect: PCC=1. (C) Mitophagy and damaged mitochondria in HPDE6-C7 cells were observed by transmission electron microscopy. Black arrows indicate normal mitochondria. Red arrows indicate damaged mitochondria and the blue arrow indicates mitophagy (magnification, x15,000; scale bar, 1.0 μm). Data were presented as the mean ± standard deviation. **P<0.01 vs. control. All experiments were repeated at least three times. RR, ruthenium red; CAE, caerulein; TOMM20, translocase of the outer mitochondrial membrane complex subunit 20; PCC, Pearson's correlation coefficient; MTG, Mito-Tracker Green; LTR, Lyso-Tracker Red.

potent inhibitor of MCU. Therefore, RR may have a significant effect on mitophagy, which is one of the important forms of autophagy. In the present study, the elevated expression of LC3-II and the decreased expression of p62 in CAE-treated cells suggested the presence and active process of autophagy. In addition, the increased colocalization of a mitochondrial marker (TOMM20) and LC3 as well as the decreased expression of TOMM20 in the present study suggested the increased level of mitophagy in CAE-treated cells. These results were supported by both the TEM and fluorescence microscopy results, where mitophagosomes were observed using TEM, and an increased colocalization of mitochondria and lysosomes was observed using fluorescence microscopy. These results indicated the presence of excessive mitophagy in PEDCs in this *in vitro* model of AP. Notably, according to the expression of TOMM20 and autophagy markers, changes in mitophagosomes and colocalization of TOMM20 and LC3 in CAE+RR-treated cells, RR was able to inhibit excessive mitophagy in PEDCs in AP. Similarly, Liu *et al* (41) found that the inhibition of the MCU attenuated excessive mitophagy and autophagic cell death by cadmium in liver cells. Yu *et al* (42) found that the inhibition of the MCU by Ru360 can inhibit hyperactivated mitophagy and protect neurocytes from ischemia/reperfusion injury. Another study has suggested that depolarized mitochondria are the initiating factor for mitophagy (43). In the present study, the MCU inhibitor RR

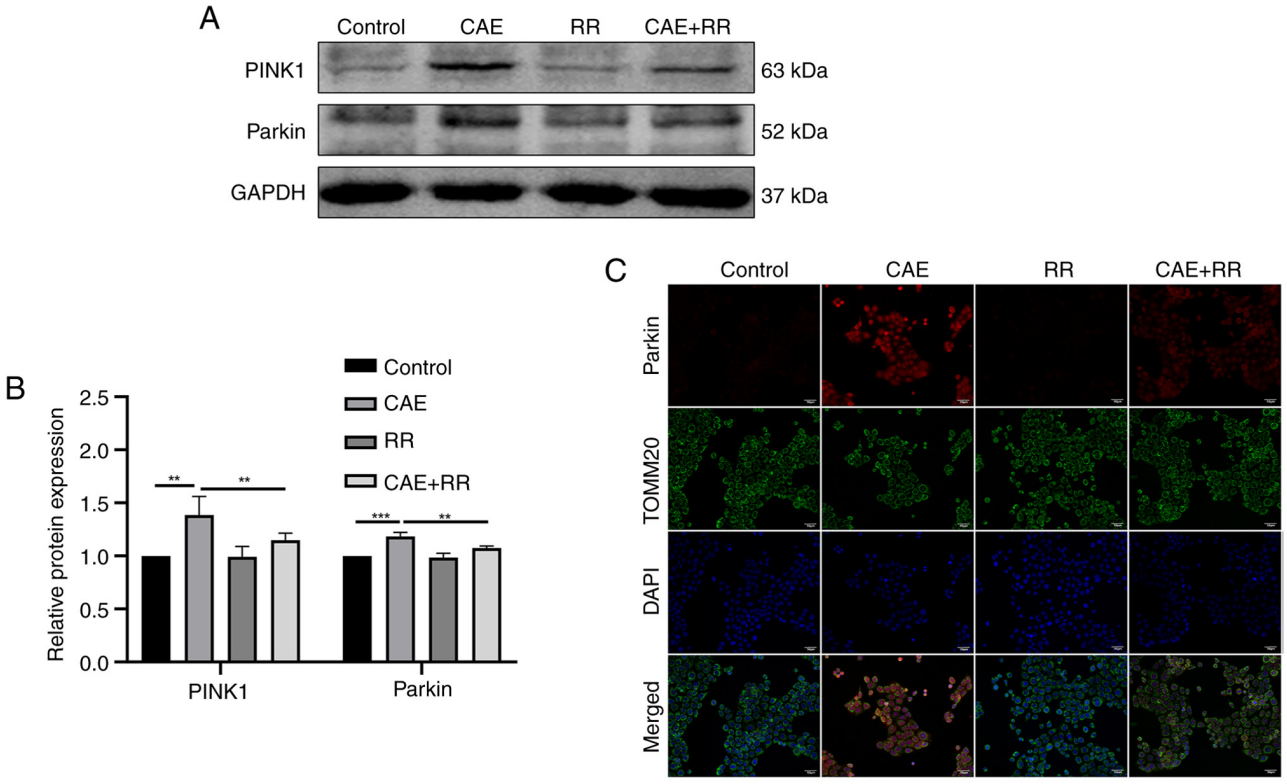

Figure 5. RR treatment decreased the expression of PINK1 and Parkin in CAE-treated HPDE6-C7 cells. HPDE6-C7 cells were treated with 10 μmol/l RR and 100 nmol/l CAE for 24 h. (A and B) Expression of PINK1 and Parkin was detected by western blotting. (C) Immunofluorescence of Parkin and TOMM20 (a mitochondrial marker) was observed by fluorescence microscopy (magnification, x200; scale bar, 50 μm). Data were presented as the mean ± standard deviation. **P<0.01, ***P<0.001 vs. control. All experiments were repeated at least three times. RR, ruthenium red; PINK1, putative kinase 1; CAE, caerulein; TOMM20, translocase of the outer mitochondrial membrane complex subunit 20.

decreased MCU expression, reduced mitochondrial Ca^{2+} overload and inhibited mitochondrial depolarization in PDECs in AP. Therefore, it can be hypothesized that the MCU can promote mitochondrial Ca^{2+} uptake and mitochondrial depolarization and further lead to mitophagy. However, whether RR exerts effects on other types of autophagy has not been reported and needs further study.

The PINK1/Parkin pathway plays an important role in the removal of dysfunctional mitochondria. First, PINK1 accumulates and is phosphorylated in the outer membrane of impaired mitochondria. Subsequently, phosphorylated PINK1 mediates Parkin translocation to the outer mitochondrial membrane and activates its ubiquitin ligase activity, causing the ubiquitination of a range of mitochondrial proteins and the formation of autophagosomes (13,43,44). Zhang *et al* (15) found that PINK1 and Parkin were elevated in the CAE-AP mouse model as well as the arginine-SAP mouse model at 24 h, but were decreased in the arginine-SAP mouse model at 48 and 72 h, suggesting that mitophagy is activated in the early stages of AP but inhibited in the late stages. The data in the present study showed that CAE promoted the expression of PINK1 and Parkin in HPDE6-C7 cells. In addition, the immunofluorescence results showed an increased translocation of Parkin to the mitochondrial outer membrane in CAE-treated cells. These changes were all reduced when the cells were treated with RR. Together, these results demonstrated that the MCU may promote mitophagy by regulating the PINK1/Parkin pathway in PDECs in AP. However, one limitation of the present study was the lack of manipulation experiments directly involving the PINK/Parkin pathway, such as the use of PINK1 inhibitors and knockout/knockdown of PINK1 or Parkin.

Either impaired mitophagy or excessive mitophagy has an important effect on cell death (45,46). The current study supported the hypothesis that mitochondrial Ca^{2+} overload by the MCU causes the accumulation of depolarized mitochondria and activates excessive mitophagy in PDECs in AP. Excessive mitophagy can lead to an imbalance in oxidative phosphorylation, oxidative stress and eventual cell death (47). Therefore, the present study provided a possible mechanism by which autophagic cell death of PDECs may disrupt the PDMB and aggravate AP. However, an important limitation of the present study was that cell death inhibitors, such as 3-MA (for autophagic cell death) (48), z-VAD (for apoptosis) (49) and Nec-1 (for necrosis) (50), were not used to detect the presence of autophagic cell death.

In addition to the inhibitor RR, the MCU activator spermine was used in the rat model of AP in our previous study (51). The results of the pre-experiment showed that spermine at different concentrations (2.5, 5.0, and 10.0 mg/kg) had no effect on the pathological score of pancreatic tissue and the amylase levels in the rat model of AP. In addition, RR effectively inhibits the MCU but also inhibits a range of other channels, including the two-pore-domain K^+ channels (tandem pore domain acid-sensitive K^+ channel 3, Twik-related K^+ channel 2 and Twik-related arachidonic acid-stimulated K^+ channel), transient receptor potential receptor vanilloid subfamily, calcium

homeostasis modulator channels, ryanodine receptor, and Piezo channels (25,52). Therefore, a superior way to investigate the role of MCU would be to use MCU knockout mice or transfection of MCU short interfering RNA. Future work will assess the regulatory effect of the MCU on mitophagy in AP using the above methods.

In conclusion, the present study suggested that MCU-associated mitochondrial Ca^{2+} overload may induce mitophagy by regulating the PINK1/Parkin pathway in PDECs in AP *in vitro*. MCU-associated mitochondrial Ca^{2+} overload and mitophagy are attractive therapeutic targets for AP in the future.

Acknowledgements

Not applicable.

Funding

The present study was supported by grants from the National Natural Science Foundation of China (grant no. 81970558) and a Scientific Research Project of the Guangxi Administration of Traditional Chinese Medicine (grant no. GXZYA20220227).

Availability of data and materials

The data generated in the present study may be requested from the corresponding author.

Authors' contributions

YL and HYY were the main contributors to the present study. YL performed experimental work, analyzed data and wrote the manuscript. HYY revised the manuscript. GDT and HYY conceived the present study and obtained funding. NM and YYQ designed the experimental procedures. MTX, XLX and LL performed cell culture and collected experimental data. YL and GDT confirm the authenticity of all the raw data. All authors read and approved the final manuscript.

Ethics approval and consent to participate

Not applicable.

Patient consent for publication

Not applicable.

Competing interests

The authors declare that they have no competing interests.

References

1. Shah AP, Mourad MM and Bramhall SR: Acute pancreatitis: Current perspectives on diagnosis and management. J Inflamm Res 11: 77-85, 2018.
2. Feng S, Wei Q, Hu Q, Huang X, Zhou X, Luo G, Deng M and Lu M: Research progress on the relationship between acute pancreatitis and calcium overload in acinar cells. Dig Dis Sci 64: 25-38, 2019.
3. Pandol SJ and Gottlieb RA: Calcium, mitochondria and the initiation of acute pancreatitis. Pancreatology 22: 838-845, 2022.
4. Hegyi P, Pandol S, Venglovecz V and Rakonczay Z Jr: The acinar-ductal tango in the pathogenesis of acute pancreatitis. Gut 60: 544-552, 2011.
5. Maleth J and Hegyi P: Calcium signaling in pancreatic ductal epithelial cells: An old friend and a nasty enemy. Cell Calcium 55: 337-345, 2014.
6. Hegyi P and Rakonczay Z Jr: The role of pancreatic ducts in the pathogenesis of acute pancreatitis. Pancreatology 15 (Suppl 4): S13-S17, 2015.
7. Wen L, Javed TA, Yimlamai D, Mukherjee A, Xiao X and Husain SZ: Transient high pressure in pancreatic ducts promotes inflammation and alters tight junctions via calcineurin signaling in mice. Gastroenterology 155: 1250-1263.e5, 2018.
8. Yang H, Liang Z, Xie J, Wu Q, Qin Y, Zhang S and Tang G: Gelsolin inhibits autophagy by regulating actin depolymerization in pancreatic ductal epithelial cells in acute pancreatitis. Braz J Med Biol Res 56: e12279, 2023.
9. Yang HY, Liang ZH, Xie JL, Wu Q, Qin YY, Zhang SY and Tang GD: Gelsolin impairs barrier function in pancreatic ductal epithelial cells by actin filament depolymerization in hypertriglyceridemia-induced pancreatitis in vitro. Exp Ther Med 23: 290, 2022.
10. Konok GP and Thompson AG: Pancreatic ductal mucosa as a protective barrier in the pathogenesis of pancreatitis. Am J Surg 117: 18-23, 1969.
11. Freedman SD, Kern HF and Scheele GA: Pancreatic acinar cell dysfunction in CFTR(-/-) mice is associated with impairments in luminal pH and endocytosis. Gastroenterology 121: 950-957, 2001.
12. Bhoomagoud M, Jung T, Atladottir J, Kolodecik TR, Shugrue C, Chaudhuri A, Thrower EC and Gorelick FS: Reducing extracellular pH sensitizes the acinar cell to secretagogue-induced pancreatitis responses in rats. Gastroenterology 137: 1083-1092, 2009.
13. Onishi M, Yamano K, Sato M, Matsuda N and Okamoto K: Molecular mechanisms and physiological functions of mitophagy. EMBO J 40: e104705, 2021.
14. Perrone M, Patergnani S, Di Mambro T, Palumbo L, Wieckowski MR, Giorgi C and Pinton P: Calcium homeostasis in the control of mitophagy. Antioxid Redox Signal 38: 581-598, 2023.
15. Zhang J, Huang W, He Q, Deng T, Wu B, Huang F, Bi J, Jin Y, Sun H, Zhang Q and Shi K: PINK1/PARK2 dependent mitophagy effectively suppresses NLRP3 inflammasome to alleviate acute pancreatitis. Free Radic Biol Med 166: 147-164, 2021.
16. Vanasco V, Ropolo A, Grasso D, Ojeda DS, García MN, Vico TA, Orquera T, Quarleri J, Alvarez S and Vaccaro MI: Mitochondrial Dynamics and VMP1-Related Selective mitophagy in experimental acute pancreatitis. Front Cell Dev Biol 9: 640094, 2021.
17. Mukherjee R, Mareninova OA, Odinokova IV, Huang W, Murphy J, Chvanov M, Javed MA, Wen L, Booth DM, Cane MC, *et al*: Mechanism of mitochondrial permeability transition pore induction and damage in the pancreas: Inhibition prevents acute pancreatitis by protecting production of ATP. Gut 65: 1333-1346, 2016.
18. Baughman JM, Perocchi F, Girgis HS, Plovanich M, Belcher-Timme CA, Sancak Y, Bao XR, Strittmatter L, Goldberger O, Bogorad RL, *et al*: Integrative genomics identifies MCU as an essential component of the mitochondrial calcium uniporter. Nature 476: 341-345, 2011.
19. Guan L, Che Z, Meng X, Yu Y, Li M, Yu Z, Shi H, Yang D and Yu M: MCU Up-regulation contributes to myocardial ischemia-reperfusion Injury through calpain/OPA-1-mediated mitochondrial fusion/mitophagy Inhibition. J Cell Mol Med 23: 7830-7843, 2019.
20. Chen Z, Zhou Q, Chen J, Yang Y, Chen W, Mao H, Ouyang X, Zhang K, Tang M, Yan J, *et al*: MCU-dependent mitochondrial calcium uptake-induced mitophagy contributes to apelin-13-stimulated VSMCs proliferation. Vascul Pharmacol 144: 106979, 2022.
21. Qin Y, Yang H, Wu Q, Xie J, Meng N, Lei Y and Tang G: Effects of inhibiting the mitochondrial calcium uniporter on the oxidative stress in rats with acute pancreatitis. China J Modern Med 32: 1-7, 2022.
22. Lerch MM and Gorelick FS: Models of acute and chronic pancreatitis. Gastroenterology 144: 1180-1193, 2013.
23. Wei B, Gong Y, Yang H, Zhou J, Su Z and Liang Z: Role of tumor necrosis factor receptorassociated factor 6 in pyroptosis during acute pancreatitis. Mol Med Rep 24: 848, 2021.

24. Wang J, Qin M, Wu Q, Yang H, Wei B, Xie J, Qin Y, Liang Z and Huang J: Effects of lipolysis-stimulated lipoprotein receptor on tight junctions of pancreatic ductal epithelial cells in hypertriglyceridemic acute pancreatitis. Biomed Res Int 2022: 4234186, 2022.
25. Marta K, Hasan P, Rodriguez-Prados M, Paillard M and Hajnoczky G: Pharmacological inhibition of the mitochondrial Ca(2+) uniporter: Relevance for pathophysiology and human therapy. J Mol Cell Cardiol 151: 135-144, 2021.
26. Colombo PM and Rascio N: Ruthenium red staining for electron microscopy of plant material. J Ultrastruct Res 60: 135-139, 1977.
27. Hajnóczky G, Csordás G, Das S, Garcia-Perez C, Saotome M, Sinha Roy S and Yi M: Mitochondrial calcium signalling and cell death: Approaches for assessing the role of mitochondrial Ca2+ uptake in apoptosis. Cell Calcium 40: 553-560, 2006.
28. Oxenoid K, Dong Y, Cao C, Cui T, Sancak Y, Markhard AL, Grabarek Z, Kong L, Liu Z, Ouyang B, *et al*: Architecture of the mitochondrial calcium uniporter. Nature 533: 269-273, 2016.
29. Wen E, Xin G, Su W, Li S, Zhang Y, Dong Y, Yang X, Wan C, Chen Z, Yu X, *et al*: Activation of TLR4 induces severe acute pancreatitis-associated spleen injury via ROS-disrupted mitophagy pathway. Mol Immunol 142: 63-75, 2022.
30. Piplani H, Marek-Iannucci S, Sin J, Hou J, Takahashi T, Sharma A, de Freitas Germano J, Waldron RT, Saadaeijahromi H, Song Y, *et al*: Simvastatin induces autophagic flux to restore cerulein-impaired phagosome-lysosome fusion in acute pancreatitis. Biochim Biophys Acta Mol Basis Dis 1865: 165530, 2019.
31. Chvanov M, Voronina S, Zhang X, Telnova S, Chard R, Ouyang Y, Armstrong J, Tanton H, Awais M, Latawiec D, *et al*: Knockout of the mitochondrial calcium uniporter strongly suppresses stimulus-metabolism coupling in pancreatic acinar cells but does not reduce severity of experimental acute pancreatitis. Cells 9: 1407, 2020.
32. Yu X, Dai C, Zhao X, Huang Q, He X, Zhang R, Lin Z and Shen Y: Ruthenium red attenuates acute pancreatitis by inhibiting MCU and improving mitochondrial function. Biochem Biophys Res Commun 635: 236-243, 2022.
33. Kirichok Y, Krapivinsky G and Clapham DE: The mitochondrial calcium uniporter is a highly selective ion channel. Nature 427: 360-364, 2004.
34. Jiang C, Shen J, Wang C, Huang Y, Wang L, Yang Y, Hu W, Li P and Wu H: Mechanism of aconitine mediated neuronal apoptosis induced by mitochondrial calcium overload caused by MCU. Toxicol Lett 384: 86-95, 2023.
35. Rodríguez-Prados M, Huang KT, Márta K, Paillard M, Csordás G, Joseph SK and Hajnóczky G: MICU1 controls the sensitivity of the mitochondrial Ca^{2+} uniporter to activators and inhibitors. Cell Chem Biol 30: 606-617.e4, 2023.
36. Biczo G, Vegh ET, Shalbueva N, Mareninova OA, Elperin J, Lotshaw E, Gretler S, Lugea A, Malla SR, Dawson D, *et al*: Mitochondrial dysfunction, through impaired autophagy, leads to endoplasmic reticulum stress, deregulated lipid metabolism, and pancreatitis in animal models. Gastroenterology 154: 689-703, 2018.
37. Shalbueva N, Mareninova OA, Gerloff A, Yuan J, Waldron RT, Pandol SJ and Gukovskaya AS: Effects of oxidative alcohol metabolism on the mitochondrial permeability transition pore and necrosis in a mouse model of alcoholic pancreatitis. Gastroenterology 144: 437-446 e6, 2013.
38. Mizushima N and Komatsu M: Autophagy: Renovation of cells and tissues. Cell 147: 728-741, 2011.
39. Barth S, Glick D and Macleod KF: Autophagy: Assays and artifacts. J Pathol 221: 117-124, 2010.
40. Liu WJ, Ye L, Huang WF, Guo LJ, Xu ZG, Wu HL, Yang C and Liu HF: p62 links the autophagy pathway and the ubiqutin-proteasome system upon ubiquitinated protein degradation. Cell Mol Biol Lett 21: 29, 2016.
41. Liu C, Li HJ, Duan WX, Duan Y, Yu Q, Zhang T, Sun YP, Li YY, Liu YS and Xu SC: MCU upregulation overactivates mitophagy by promoting VDAC1 dimerization and ubiquitination in the hepatotoxicity of cadmium. Adv Sci (Weinh) 10: e2203869, 2023.
42. Yu S, Zheng S, Leng J, Wang S, Zhao T and Liu J: Inhibition of mitochondrial calcium uniporter protects neurocytes from ischemia/reperfusion injury via the inhibition of excessive mitophagy. Neurosci Lett 628: 24-29, 2016.
43. Shirihai OS, Song M and Dorn GW II: How mitochondrial dynamism orchestrates mitophagy. Circ Res 116: 1835-1849, 2015.
44. Nguyen TN, Padman BS and Lazarou M: Deciphering the molecular signals of PINK1/Parkin mitophagy. Trends Cell Biol 26: 733-744, 2016.
45. Sidarala V, Pearson GL, Parekh VS, Thompson B, Christen L, Gingerich MA, Zhu J, Stromer T, Ren J, Reck EC, *et al*: Mitophagy protects β cells from inflammatory damage in diabetes. JCI Insight 5: e141138, 2020.
46. Rademaker G, Boumahd Y, Peiffer R, Anania S, Wissocq T, Liegeois M, Luis G, Sounni NE, Agirman F, Maloujahmoum N, *et al*: Myoferlin targeting triggers mitophagy and primes ferroptosis in pancreatic cancer cells. Redox Biol 53: 102324, 2022.
47. Kang SU, Kim DH, Lee YS, Huang M, Byeon HK, Lee SH, Baek SJ and Kim CH: DIM-C-pPhtBu induces lysosomal dysfunction and unfolded protein response-mediated cell death via excessive mitophagy. Cancer Lett 504: 23-36, 2021.
48. Pasquier B: Autophagy inhibitors. Cell Mol Life Sci 73: 985-1001, 2016.
49. Green DR: Caspase activation and inhibition. Cold Spring Harb Perspect Biol 14: a041020, 2022.
50. Cao L and Mu W: Necrostatin-1 and necroptosis inhibition: Pathophysiology and therapeutic implications. Pharmacol Res 163: 105297, 2021.
51. Qin Y YH and Tang G: Effects of activated mitochondrial calcium uniporter on acute pancreatitis induced by caerulein in rats. Electronic Journal of Clinical Medical Literature 8: 8-11, 2021.
52. Ma J: Block by ruthenium red of the ryanodine-activated calcium release channel of skeletal muscle. J Gen Physiol 102: 1031-1056, 1993.